

Automatic interpretation of cod otoliths using deep learning

Endre Moen^{1*}, Rune Vabø¹, Come Denechaud¹, Ketil Malde^{1,2},

1 Institute of Marine Research, Bergen, Norway

2 Department of Informatics, University of Bergen, Norway

* endre.moen@hi.no

Abstract

The age of individual cod (*Gadus morhua*) is determined by manually examining the layered structure of otoliths, a calcium carbonate structure of the inner ear.

Image-based methods have been tried to age otoliths with varying results, but recent developments in automatic image analysis techniques are promising. The objective of this paper is to investigate the accuracy in aging broken otolith images on state-of-the-art convolutional neural networks.

Introduction

Information on fish age constitutes one of the most important biological variables, which is used in the investigations of life history (e.g. growth, sexual maturation) and population dynamics Campana [2001]

– The need for more Automated analysis. On the future of data analysis. – On the importance of determining age distributions for fisheries and ecosystem management. – How Cod otoliths are measured manually. The importance of otoliths for age determination of various species. Specifics about cod. – Related work. Halibut otoliths. Salmon scales. The Greeks. Knowledge of fish age structure is central to the study of fish and stock dynamics. It informs on population growth and mortality and, with size distribution, is one of the main criteria used for determining the health of exploited

populations and monitoring the effects of selective fishing (Hidalgo et al., 2011; Brunel and Piet, 2013). Changes in the age distribution can track significant changes in population structure, such as a particularly strong year-class skewing the distribution (Reglero and Mosegaard, 2006), or the gradual truncation of older age classes as selective fishing mortality removes larger individuals (Siskey et al., 2016). Hard structures such as scales and otoliths are used worldwide as one of the primary sources of fish age estimates, due to their ability as natural physiological and environmental recorders to form regular, temporally resolved growth increments at the daily and annual levels (Campana, 2001; Francis and Campana, 2011; Albuquerque et al., 2019). While age is inferred from the “simple” counting of annual increments, the interpretation of this zonation pattern is species or even population-specific (Høie et al., 2009) and is based on precise knowledge of the timing of zone formation and of the correct identification of true and false zones (Panfili et al., 2002). This process therefore requires specific expertise and is subject to uncertainties in both between-reader precision and “true” age accuracy (Francis and Campana, 2011). Because those estimates are central to stock assessment, ageing errors or wrong interpretation of otolith zonation can have dramatic effects on the evaluation of fish biology and consequently stock size and structure (Tyler et al., 1989; Beamish and McFarlane, 1995; Ragonese, 2018). Otolith reading is also time and resource consuming. Training of expert readers can take up to several years depending on the species, and otoliths often undergo a long processing phase before the final age estimates can be produced (Carbonara and Follesa, 2019). This is particularly true for demersal fish species, like Atlantic cod (*Gadus morhua*), that have large opaque otoliths that can't be read whole and need to be prepared. These routines vary between populations and institutes and range from direct reading of broken otoliths under a magnifying glass, to embedding, thin sectioning and finally imaging of the sections under a microscope. There has been a variety of methods proposed to automatically interpret otoliths, which range from one-dimensional data analysis like intensity transects (Mahé, 2009) to the more recent effort toward developing machine learning (ML) frameworks (Moen et al., 2018; Politikos et al., 2021). Despite fast progress the results remain mixed and often yield lower precision and consistency than those obtained by trained human readers, which limits the application of automated methods in real conditions. However, one aspect that is often under considered by such studies

are the practical time and cost benefits that implementing a functional ML framework would provide. As noted by Fisher and Hunter (2018) in their review of digital techniques for otolith analysis, “costs for human and machine ageing systems are broadly similar since a large part of the cost is associated with preparing the otolith sections”. As such, the net benefit of automated ageing routines is directly dependent on the ability to scale performance using a comparatively smaller number of samples than human readers or, alternatively, to train them on “rougher” data that can be produced faster and at a more efficient cost. MORE ON CNN ETC? In this study, we develop a deep learning network for estimating Atlantic cod age using multi-exposure images of broken otoliths set in place using simple plasticine. More on methods. Our results are positive and show the potential for developing automated pipelines that require minimum processing and could be able to produce near at-sea age estimates.

Method and materials

Data Collection

We sampled a data set of 5150 cod otolith images, which has been collected on different cruises and read by otolith experts. The images are taken during cruises in the period 2012-2018 conducted by Institute of Marine Research (IMR). There are six images with three light exposures and one rotation. The expert readers has varied during this time period as has the configuration for photographing the otoliths.

Figure 1. Otolith from 2016, read age: 6. With light exposure: medium, low, high, then rotated 180 degrees and three new images



The images is of size 3744 x 5616 which are re-scaled for training to between 384x384 to 512x512. The image light exposure varies depending on light condition outside, and

are stored in the property 'ExposureTime' of the JPG file. Typically the exposure order
72 is middle, dark, or light then a rotation of 180 degrees, and then middle, light, dark
73 again. But the order might change, and the given order is recovered by reading the
74 metadata property of the jpeg and sorting the exposure time.
75

The otoliths are prepared for imaging by breaking them. The process also involves a
76 camera setup, a folder structure referencing age, survey and station number, lighting
77 setup, mounting of camera, and finally camera capture. More information about this
78 process can be found in S.C. Myers [2019]
79

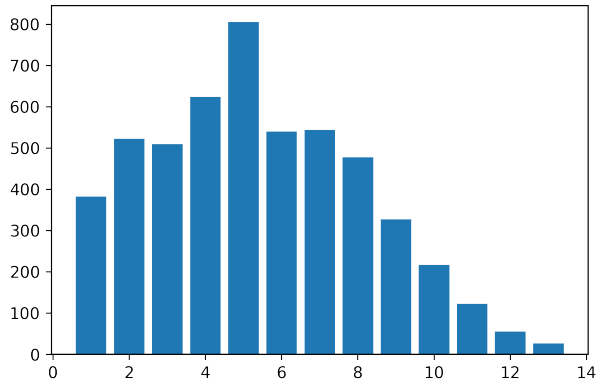


Figure 2. Age distribution of all 5150 images

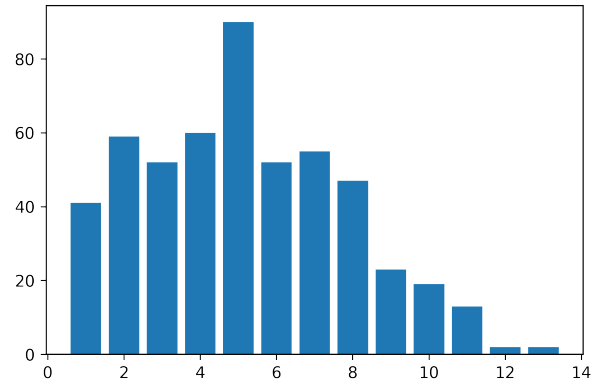


Figure 3. Age distribution of 515 images from the test set

Preprocessing and augmentation

To create a large data set with millions of images needed to evaluate the models, we use
80 image augmentation. Image augmentation has made it possible to do deep CNN
81 training on smaller data sets (kri). By using this technique it is possible to create
82

millions of training images.

The augmentation methods that we use are rotation by 0 to 360 degrees, and reflection by the vertical (or horizontal) axis. This can be done without loss of information. Also the age reading is agnostic to orientation.

No other augmentation techniques was used like cropping, shifting or shearing as it can result in loss of age structure information.

The augmented data set can produce $360*2*5150 = 3.708.000$ possible images.

Depending on the augmentation factor and the number of images in a training cycle, the model will likely never see the same image twice.

The data has been split into train and test-set with 10 % test-set, 9 % validation and 81 % training-set. Training has been done on the 90 % of the data set, 4635 images, with 10-fold split producing 10 models. While predictions are made on the 515 images in the test set. The final prediction is an ensemble prediction on the given model recorded as the expectation on predictions on the test set from the 10 models.

Figure 4. Otolith from 2013, read age: 6. With light exposure: medium, low, high, and expectation per channel of the three exposures.



Training the Convolutional neural networks

There are two families of models used, EfficientNet B4-B6 (?) from Tensorflow (2) with a Keras (4) implementation plus weights, and a PyTorch (?) implementation of EfficientNet V2 medium, Large and Xtra-Large (6) implementation with weights from Timm(9). Weights are ImageNet (5) weights, which is another prerequisite when working with small data sets, in addition to augmentation. The image size varies between 380 and 528 for EfficientNet Bx, and 384 for EfficientNetV2 size medium, large and xtra-large. While test-set size prediction has been done both on 384 and larger

resolutions 480 and 512 as described in the paper. To investigate the image-taking
106 protocol described in (7) we have is also training on 9-channel images. Three images are
107 stacked to produce a 9-channel. Using Timm(9) the imagenet weights are duplicated on
108 the input layer to accommodate 9 channels. The 3 images used are of dark, medium and
109 light exposure of the first orientation.
110

EfficientNetV2 has been modified slightly because the objective is regression as
111 opposed to classification. The output layer of EfficientNetV2 becomes input to a
112 Multi-Layer Perceptron (MLP) of 256 and 32 layers and then to a linear activation
113 function which is the predicted age. More specifically; the 1280 layers output from
114 EfficientNetV2 is input to 256 layer-MLP, then a leakyRelu (10) then 32 layer-MLP,
115 another leakyRelu, then a linear activation function is the output. This outperformed a
116 linear activation on the 1280 layers from EfficientNetV2, likely because we are doing a
117 regression.
118

We train and tune EfficientNet B4, B5, B6 (8), EfficienNetV2 medium, large (8),
119 and xl. The test results from top models are ensembled to produce the final prediction.
120

Hyper-parameter tuning is an important step when working with a new dataset and
121 architecture. Some hyper-parameters that as been tuned are batch size, learning rate,
122 k-fold size, weight decay, step size, number of epochs, early stopping, and patience. To
123 keep track of all these parameters, a config.json file has been written for each model
124 trained, and the exact configuration can be found the the results section of the github
125 page of this project
126

(<https://github.com/emoen/Deep-learning-for-regression-of-cod-otoliths>)
127

Ensemble of ensembles 128

As previously mentioned, the results recorded per model is an ensemble of 10 models
129 trained on 10-fold split of the training data set. Typically the ensemble prediction is
130 better than any single fold prediction. Ensembles are better because they improve
131 performance. An ensemble can make better predictions and achieve better performance
132 than any single contributing model, just as more experts will produce higher accuracy
133 in predicting a single otolith. Robustness; An ensemble reduces the spread or dispersion
134 of the predictions and model performance. This result can be improved further by
135

taking ensemble predictions of multiple models as prediction on the test set. We look at
136 all ensembles from tuple predictions consisting of 2 models, which produces an ensemble
137 of 20 models, to ensemble of all models which produces an ensemble consisting of 210
138 models. By choosing the best model we are over fitting to the test-set, but selecting a
139 subset of the best of these ensembles should produce a candidate ensemble of ensemble
140 which will produce the best prediction on a test-set holdout set.
141

Evaluation metric

The primary metric used for training the models is mean squared error (MSE) while the
142 primary metric used for evaluating the models is Accuracy. Accuracy is obtained by
143 rounding the floating point number predictions to nearest integer and comparing the
144 age classification against the true labels. To reach human level accuracy a score of 85%
145 or higher is required (?).
146

Results

We have conducted a series of experiments on the EfficientNet family of CNNs, with
149 different hyper-parameters and on images with light exposures from the set light,
150 medium, dark. Training has been done on the 10-fold cross validation set which
151 produced 10 models. An ensemble of the best models produced the best accuracy score
152 in table 1 and MSE in table 1. It can be observed that in the efficientNetV1 family,
153 larger networks has better MSE, while accuracy is more fluctuating. A similar pattern
154 can be observed for the efficientNetV2 networks. However it seems like efficientNetV1
155 is better than V2, unlike the results observed on ImageNet.
156

Table 1. Accuracy by light exposure and CNN architectures

MSE:light/CNN	B4	B5	B6	Medium	Large	Xtra Large
min	72.8	74.4	73.4	67.0*	-	-
medium	-	-	74.4	72.4	71.8	-
max	-	-	-	-	-	-
9 channels	-	-	-	-	71.7	-

Table 2. MSE by light exposure and CNN architectures

ACC:light/CNN	B4	B5	B6	Medium	Large	Xtra Large
min	.277	.277	.272	.331*	-	-
medium	-	-	.262	.292	.280	-
max	-	-	-	-	-	-
9 channels	-	-	-	-	.281	-

**Figure 5.** Sample of 25 predictions on a fold of training on EfficientNetV2 size medium with minimum light exposure, left number is prediction, and right number is age read

We compare the 10 fold prediction accuracy of all the models in a box plot in figure 159, and for MSE in 11. The metric for each of the 10 folds are given by the box plot, and 160 the red line is the ensemble accuracy or MSE. The ensemble metric is either better than 161 all the folds or in the upper quantile. 162

By comparing the models on MSE we can see that larger models are better, e.g B6 163 has higher mean than B5 and B4, and large is better than medium. We also see that 164 the EfficientNetV2 networks has higher mean than mean than the first generation 165 EfficientNet. However, this is not true for the ensemble predictions (red line) nor for the 166 mean or ensemble mean of the accuracy. We can also see that the effect of adding 3 167 images - 9 channels on the model is that the variance is reduced. 168

The box-plots are produced from the fold metrics:

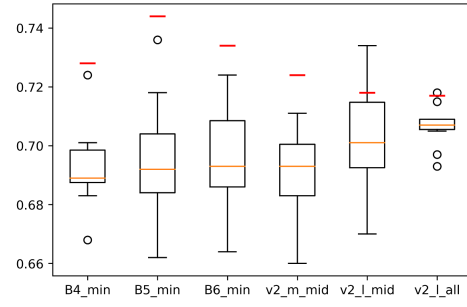


Figure 6. Accuracy score of 5 models and red line is ensemble prediction accuracy

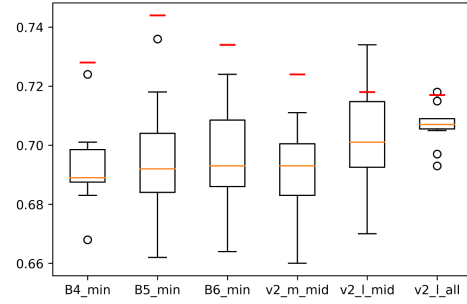


Figure 7. MSE score of 5 models and red line is ensemble prediction MSE

Table 3. MSE per CNN and per fold

CNN/fold	1	2	3	4	5	6	7	8	9	10	mse
B4, min	.320	.318	.3.	.313	.322	.314	.315	.316	.3.	.3.	.277
B4, middle											
B4, max											
B5, min	.324	.322	.325	.336	.291	.314	.320	.331	.33	.317	.277
B5, middle											
B5, max											
B6, min	.325	.329	.334	.293	.312	.290	.320	.3.	.276	.3.	.272
B6, middle	.323	.3.	.312	.268	.294	.266	.3.	.311	.278	.289	.262
B6, max											
medium, min											
med., mid.	.321	.377	.332	.285	.285	.325	.311	.348	.295	.373	.292
medium, max											
medium, all											
large, min											
large, middle	.3.	.281	.299	.318	.282	.3.	.280	.334	.3.	.310	.280
large, max											
large, all	.292	.289	.289	.326	.3.	.327	.283	.30	.335	.295	.281
xl, min											
xl, middle											
xl, max											
xl, all											

Table 4. Accuracy per CNN and per fold

CNN/fold	1	2	3	4	5	6	7	8	9	10	acc
B4, min	69.9	68.9	68.7	68.3	68.9	70.1	69.7	66.8	68.9	72.4	72.8
B4, middle											
B4, max											
B5, min	71.8	69.1	69.3	66.8	73.6	70.7	66.2	68.3	69.5	68.7	74.4
B5, middle											
B5, max											
B6, min											
B6, middle	68.3	68.5	66.4	72.4	70.7	70.9	69.3	69.3	72	68.9	73.4
B6, max	68.5	69.9	67.6	73.6	72.8	72	68	69.3	72	71.1	74.4
medium, min											
med., mid.	68.7	67.6	68.3	71.1	70.1	70.5	69.9	68.3	69.9	66	72.4
medium, max											
medium, all											
large, min											
large, middle	69.7	73.4	69.1	67	71.8	69.9	72.6	68.2	70.5	70.3	71.8
large, max											
large, all	70.9	70.7	70.5	70.7	71.5	69.3	70.7	71.8	69.7	70.9	71.7
xl, min											
xl, middle											
xl, max											
xl, all											

Prediction by age class and residuals

170

The figures below shows the predictions per age group on the test-set. We can see that 171
the prediction follows a linear trend $y = x$ except for the 2-3 last years. We also see the 172
same on the residual plots 173

Lets look at the scatter-plot of the errors which causes misclassifications. 174

Ensemble of ensembles

175

We search the space of ensemble of ensemble predictions which are given by $\sum_{k=1}^N \binom{N}{k}$ 176
where $N = 22$ and $k \in 1..N$ 177

Table 5. Accuracy/MSE pr ensemble of ensemble. Eoe1 is ensemble of ensemble of all models, Eoe2 is for B4, B5 and B6, and Eoe3 is Eoe2 plus efficientNetV2 medium.

score/ensemble	eoe1	eoe2	eoe3
Acc	75.9	76.1	76.9
MSE	.247	.248	.248

178

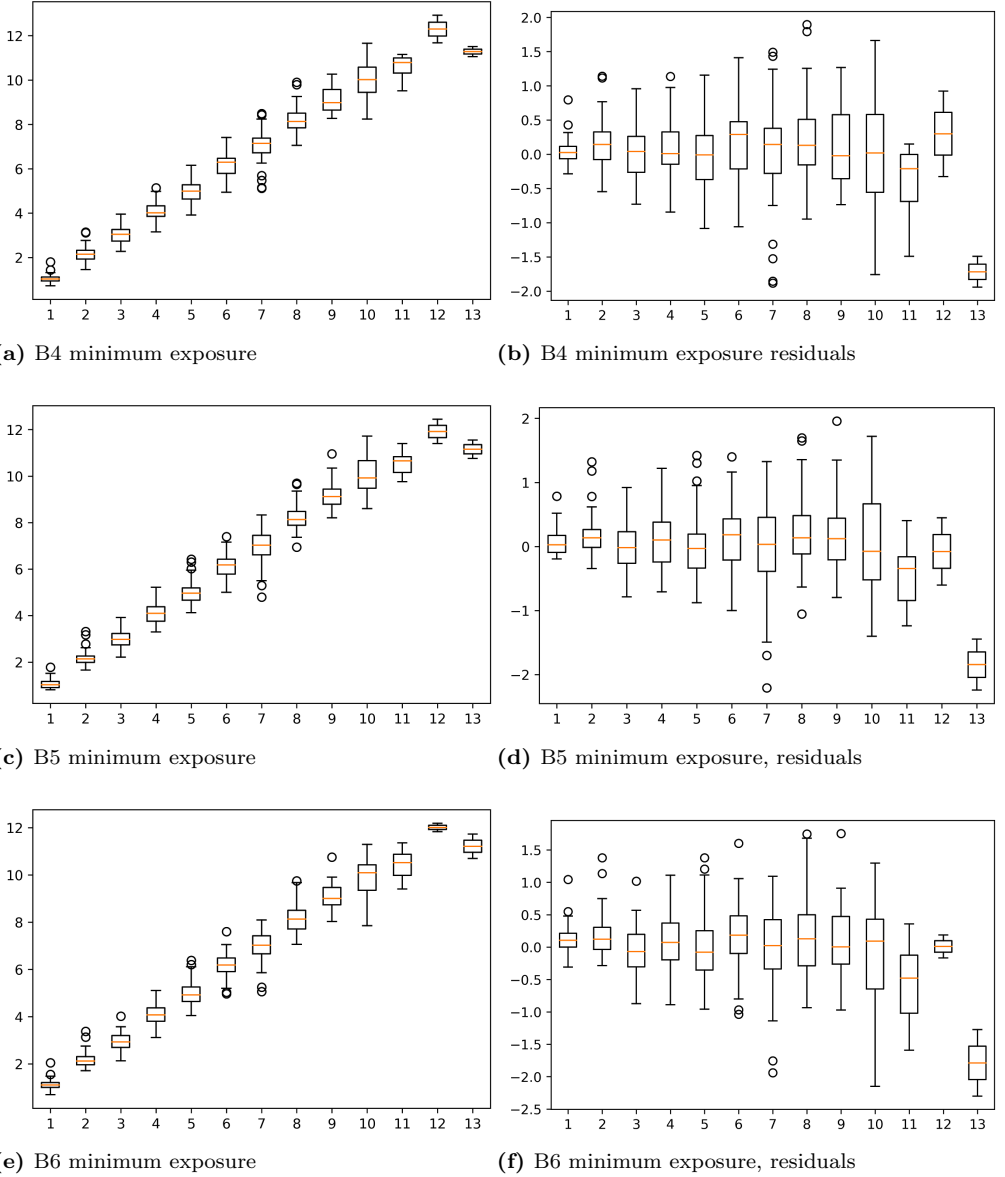
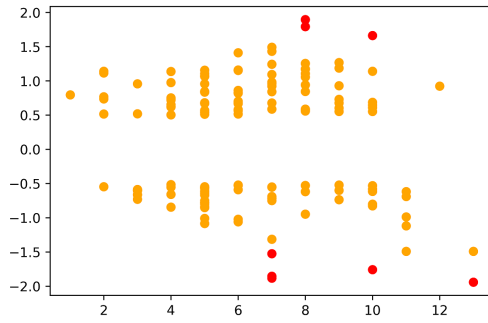
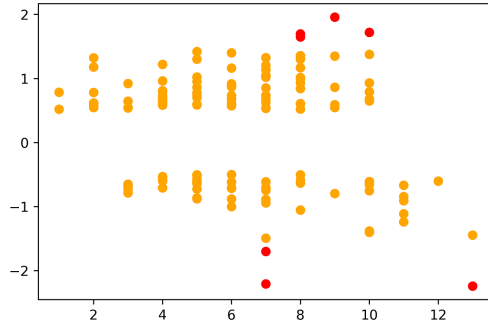


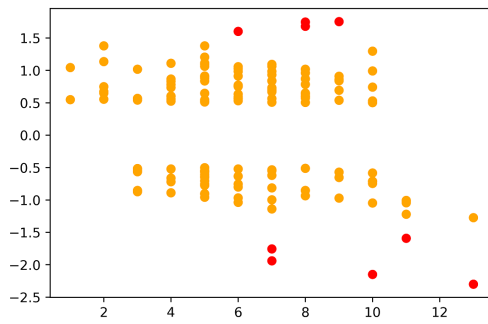
Figure 8. Comparing the models, looking at age per age class, and the residuals per prediction



(a) B4 minimum exposure



(b) B5 minimum exposure



(c) B6 minimum exposure

Figure 9. Comparing the models, looking at age per age class, and the residuals per prediction

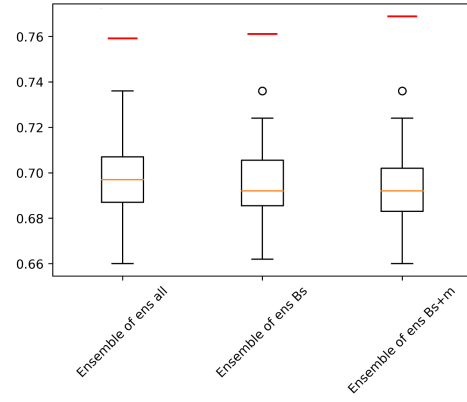


Figure 10. Ensemble of ensemble:
accuracy of the 3 best models

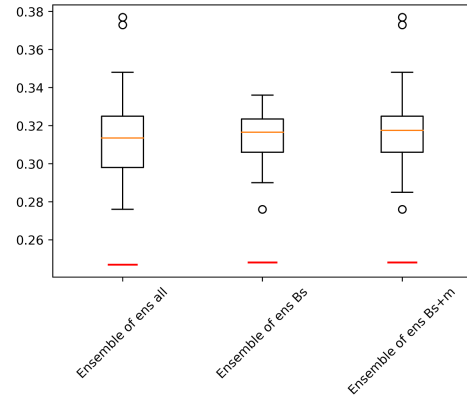


Figure 11. Ensemble of ensemble: mse of
the 3 best models

Outliers

Looking at figure (x) we can see that the model under predicts the age of older otoliths. 180
 This pattern is especially observable for individuals read as 15 years and older. The 181
 oldest predication is 18 years while the test set contains individuals as old as 22 years. 182
 To better understand the bias, figure 11 shows the 4 largest outliers from the test set 183
 which come from two pairs 184

Figure ?? are the most commonly misclassified images with greatest magnitude of 185
 error. 186

Figure 12. The most common images miss predicted with more than 1.5 years



Discussion

During initial training we trained a B4 network on ca 2000 images and obtained an accuracy of ca 60%, later another 3000 images was added and the same network was trained on ca 5000 images which resulted in accuracy of ca 70%. It could be interesting to investigating if adding another 3-5000 images would increase the accuracy to 80%.

References

References

- kri.
2. Abadi, M., Agarwal, A., Barham, P., Brevdo, E., Chen, Z., Citro, C., Corrado, G. S., Davis, A., Dean, J., Devin, M., et al. (2016). Tensorflow: Large-scale machine learning on heterogeneous distributed systems. *arXiv preprint arXiv:1603.04467*.
 3. Campana, S. (2001). Accuracy, precision and quality control in age determination, including a review of the use and abuse of age validation methods. *Journal of fish biology*, 59(2):197–242.
 4. Chollet, F. and others (2018). Keras 2.1.3. <https://github.com/fchollet/keras>.
 5. Deng, J., Dong, W., Socher, R., Li, L.-J., Li, K., and Fei-Fei, L. (2009). Imagenet: A large-scale hierarchical image database. In *Proceedings of IEEE Conference on Computer Vision and Pattern Recognition*, pages 248–255. IEEE.

6. Mingxing Tan and, Q. V. L. (2021). Efficientnetv2: Smaller models and faster
205 training. *CoRR*, abs/2104.00298.
206
7. S.C. Myers, A. Thorsen, J. G. K. M. N. H. (2019). An efficient protocol and data
207 set for automated otolith image analysis. *GeoScience Data Journal*.
208
8. Tan, M. and Le, Q. V. (2019). Efficientnet: Rethinking model scaling for
209 convolutional neural networks. *CoRR*, abs/1905.11946.
210
9. Wightman, R. (2019). Pytorch image models.
211
<https://github.com/rwightman/pytorch-image-models>.
212
10. Xu, B., Wang, N., Chen, T., and Li, M. (2015). Empirical evaluation of rectified
213 activations in convolutional network. *CoRR*, abs/1505.00853.
214